

Derived faunivores are the forerunners of major synapsid radiations

Received: 22 April 2022

Accepted: 6 August 2023

Published online: 05 October 2023

 Check for updates

Spencer M. Hellert ^{1,2,7}✉, David M. Grossnickle ^{3,4,7}, Graeme T. Lloyd ⁵, Christian F. Kammerer ⁶ & Kenneth D. Angielczyk ¹

Evolutionary radiations generate most of Earth's biodiversity, but are there common ecomorphological traits among the progenitors of radiations? In Synapsida (the mammalian total group), 'small-bodied faunivore' has been hypothesized as the ancestral state of most major radiating clades, but this has not been quantitatively assessed across multiple radiations. To examine macroevolutionary patterns in a phylogenetic context, we generated a time-calibrated metephylogeny ('metatree') comprising 1,888 synapsid species from the Carboniferous through the Eocene (305–34 Ma) based on 269 published character matrices. We used comparative methods to investigate body size and dietary evolution during successive synapsid radiations. Faunivory is the ancestral dietary regime of each major synapsid radiation, but relatively small body size is only established as the common ancestral state of radiations near the origin of Mammaliaformes in the Late Triassic. The faunivorous ancestors of synapsid radiations typically have numerous novel characters compared with their contemporaries, and these derived traits may have helped them to survive faunal turnover events and subsequently radiate.

Examining the catalysts of evolutionary radiations is critical for elucidating the origins of Earth's biodiversity. Research on evolutionary radiations is often performed from the perspective of the descendent lineages (including extant taxa), assessing the phylogenetic relationships, morphological disparity through time and speciation rates of diverging lineages^{1–4}. In contrast, there has been less focus on the forerunners of evolutionary radiations and few quantitative tests of shared ecomorphological traits among ancestral taxa of multiple radiations⁵. One observed pattern is that early lineages of radiating clades tend to be smaller in body size than many descendant lineages^{6,7}. Because there is covariance between body size and some ecological traits such as diet^{8–16}, selective extinctions of taxa of specific sizes or ecological traits is likely to result in surviving lineages with shared traits. Further, Cope's 'law of the survival of the unspecialized'^{6,17–22} posits that ecologically unspecialized taxa (that is, generalists) may commonly survive when more specialized lineages perish during extinction events, resulting in

unspecialized lineages being the progenitors of subsequent radiations. These considerations suggest that there may be stereotyped ancestral ecomorphotypes at the base of evolutionary radiations.

Here we test whether 'small-bodied faunivore' is the ancestral ecomorphotype of lineages that gave rise to major radiations within Synapsida. For patterns of body size, our aim is to assess whether the ancestral taxa of radiations are consistently small bodied relative to descendant taxa. Synapsid history extends ~320 Myr (ref. 23) and is marked by the iterative evolution of ecomorphologically diverse clades, culminating in extant taxa (monotremes, marsupials, placentals) displaying spectacular morphological and ecological diversity. Conventional wisdom states that throughout synapsid history, relatively small-bodied faunivores are dominant early in evolutionary radiations and they give rise to ecologically diverse clades^{6,24–28}. Previous work has shown that small-bodied faunivore is the dominant ancestral ecomorphotype early in mammaliaform radiations (see ref. 28 and citations therein),

¹Negaunee Integrative Research Center, Field Museum of Natural History, Chicago, IL, USA. ²Department of Science and Mathematics, Columbia College Chicago, Chicago, IL, USA. ³Department of Biology, University of Washington, Seattle, WA, USA. ⁴Natural Sciences Department, Oregon Institute of Technology, Klamath Falls, OR, USA. ⁵Independent Researcher, Amble, UK. ⁶North Carolina Museum of Natural Sciences, Raleigh, NC, USA.

⁷These authors contributed equally: Spencer M. Hellert, David M. Grossnickle. ✉e-mail: shellert@fieldmuseum.org

with the pattern of increasing body size diversity in crown mammal groups often used to test Cope's rule^{7,29,30}, or 'Alroy's Axiom'³¹, which states that lineages tend to evolve towards larger body size. However, there has been no rigorous test of whether this pattern applies across the entire evolutionary history of Synapsida.

To test the hypothesis that relatively small-bodied faunivores are the forerunners of most synapsid radiations, we examine macroevolutionary patterns in body size and diet (Fig. 1a). It has been challenging to test the small-bodied faunivore hypothesis in a way that encompasses all of synapsid history, in part because the necessary infrastructure, namely a comprehensive synapsid phylogeny, was unavailable. Therefore, we generated a time-calibrated metatree of synapsid species that focuses on taxa from the Carboniferous through the Eocene (305–34 Ma), incorporating 269 published morphological character matrices. We used the metatree in conjunction with jaw lengths (as a proxy for body size) and diet reconstructions for 404 synapsid species to investigate ecomorphological patterns during successive synapsid radiations. For our primary analyses, we analysed five temporally successive major radiations: (1) non-therapsid pelycosaurs (hereafter 'pelycosaurs'), (2) non-cynodont therapsids (hereafter 'therapsids'), (3) non-mammaliaform cynodonts (hereafter 'cynodonts'), (4) non-therian mammaliaforms (hereafter 'mammaliaforms') and (5) therians (eutherian-placental and metatherian-marsupial lineages). Each of these radiations is marked by considerable ecological diversification (thus, hereafter we refer to them as 'ecological radiations'), with descendent lineages achieving a broad diversity of body masses and diets^{23,27,28} (Supplementary Methods). We further examined radiations at a phylogenetically finer scale in supplementary analyses. Our results shed new light on the forerunners of synapsid radiations and inform our understanding of evolutionary transitions that influenced the rise of extant mammals.

Results

Metatree

Our time-calibrated metatree ('metatree'; sensu ref. 32) includes 1,888 synapsid species that are primarily from the Carboniferous through the Eocene (305–34 Ma). The tree is based on 269 published character matrices (listed in Supplementary Table 6). The metatree is a comprehensive species-level phylogeny for non-mammaliaform synapsids; it incorporates all published character matrices that focus on non-mammaliaform synapsids (as of July 2021). Further, it includes 57 mammaliaform- and mammal-focused matrices and samples ~525 mammaliaforms and mammals. The metatree was pruned to the 404 species for which we had jaw length data. See the Supplementary Information for additional discussion of the metatree, including the synapsid sample and tree topology, and for a version of our pruned phylogeny with tip labels (Extended Data Figs. 1–5 and Supplementary Fig. 1).

Body size patterns

Among the five major ecological radiations, correlation analyses and regressions (ordinary least squares (OLS) and phylogenetic generalized least squares (PGLS)) of jaw lengths (a proxy for body size) against patristic distances (see Methods for a detailed definition of patristic distance) were both only statistically significant for therians (Table 1, and Supplementary Tables 2 and 5). In addition, the OLS (but not PGLS) linear regression was statistically significant for mammaliaforms. Therians and mammaliaforms both displayed a positive trend in body size evolution with time (Fig. 2), and their ancestral body sizes are reconstructed as being especially small (Table 1, and Supplementary Tables 3 and 5). Pelycosaurs and cynodonts showed a slight negative trend in body size with time (Fig. 2). Thus, there was no common trend in body size evolution among all five radiations.

The lack of consistent trends for non-mammaliaform radiations is reflected by a conflicting mixture of patterns among the subclades within each radiation (Extended Data Figs. 3–6, and Supplementary

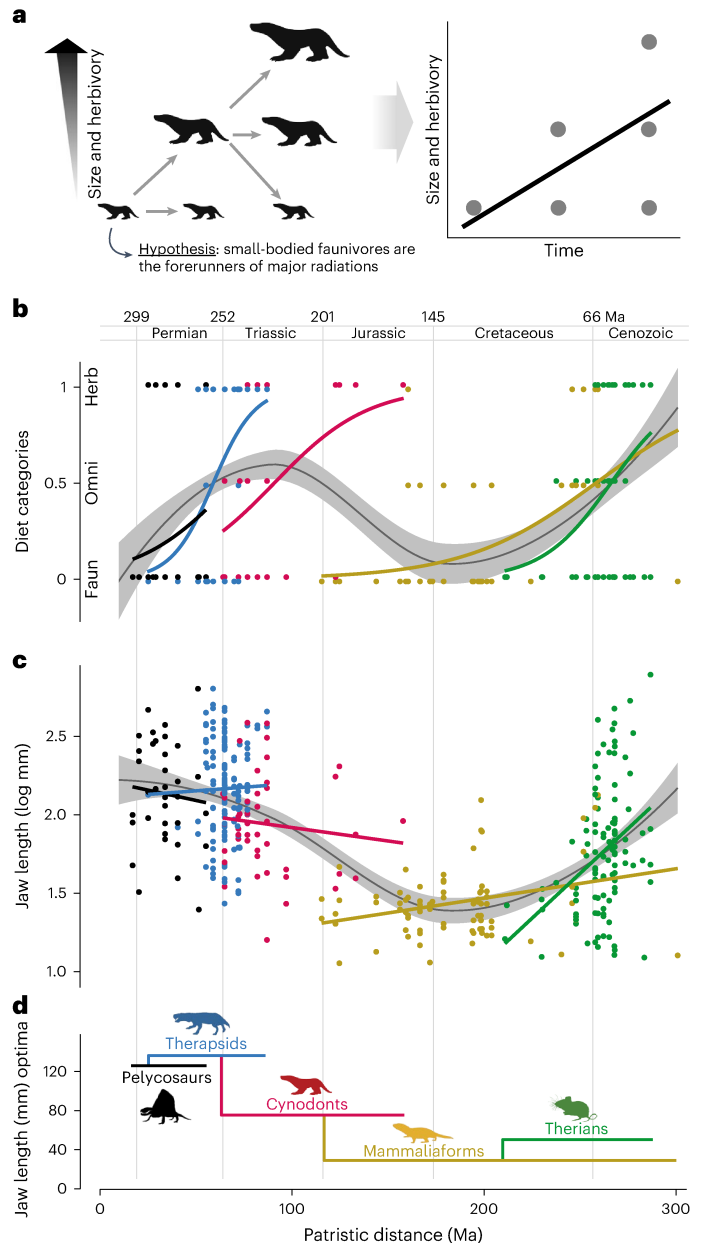


Fig. 1 | Testing the hypothesis that small faunivores are the forerunners of synapsid radiations using diet and body size patterns through time.

a, Conceptual illustration of the tested hypothesis (left) and predicted patterns of regression results (right). Diet was quantified by assigning taxa to numeric categories and jaw length was used as a proxy for body size. **b, c**, Diet (**b**) and jaw lengths (**c**) for all synapsids in our sample are plotted against patristic distance. The regression lines in **b** and **c** represent quasibinomial (for diet) and linear (for jaw lengths) models for each of the groups of taxa that make up the major synapsid ecological radiations (see Fig. 2). See Extended Data Fig. 6 for versions of **b** and **c** that include regression lines of smaller subclades analysed in this study. The grey curves are LOESS-fitted (locally weighted scatterplot smoothing) regression curves and the associated bands are 95% confidence intervals. **d**, The jaw length optima from the fitted five-peak Ornstein–Uhlenbeck evolutionary model (see Results), which treats each major radiation as a different model regime. Models were fit to \log_{10} -transformed jaw lengths, but we back-transformed the length optima here for ease of interpretation. The silhouettes in **d** are by J. Iza (therapsid), C. Axon (cynodont) and E. Newham (mammaliaform). They were obtained from www.phylopic.org and are available via license CC0.0. faun, faunivory; herb, herbivory; omni, omnivory.

Tables 1 and 2). For pelycosaur subclades, the only significant trend in body size through time was within Sphenacodontidae, which experienced a positive trend (Supplementary Table 1 and Extended

Table 1 | Summary statistics for body size (jaw length) and dietary analyses of the major synapsid radiations

Radiation	Body size (jaw length) analyses								Diet analyses				
	Jaw lengths (mm)			Linear regressions			Kendall rank correlation		ASR	Quasibinomial regression		Kendall rank correlation	
	Median	Range	ASR	t-stat	P value	r ²	tau	P value	Faunivory likelihood	t-stat	P value	tau	P value
Pelycosaur	135.15	24.83–634.98	100.60	-0.512	0.612	0.008	-0.081	0.501	>0.999	1.047	0.303	0.193	0.184
Therapsids	295.50	27.12–636.38	134.73	0.276	0.783	0.001	-0.044	0.452	>0.999	3.366	0.001	0.223	0.002
Cynodonts	87.43	15.90–385.89	103.26	-0.783	0.438	0.014	-0.079	0.450	0.772	2.459	0.018	0.255	0.034
Mammaliaforms	26.93	11.30–133.59	29.06	2.673	0.009	0.086	0.090	0.244	>0.999	3.310	0.001	0.317	0.001
Therians	52.62	12.28–781.30	24.13	4.099	<0.001	0.135	0.253	<0.001	0.997	3.405	0.001	0.219	0.004

For the linear regressions and Kendall rank correlation coefficient analyses, data were analysed against patristic distances. Before analyses, jaw lengths (proxies for body sizes) were \log_{10} -transformed and taxa were assigned to one of three dietary categories (1, faunivore; 2, omnivore; 3, herbivore). Ancestral-state reconstructions (ASRs) are at the basal node of each radiation. Jaw length ASRs were calculated using \log_{10} -transformed jaw lengths, but we back-transformed the data for ease of interpretation. The diet ASRs are the scaled likelihoods for faunivory. Note that the first four radiations are paraphyletic grades. Significance tests are two-tailed and not adjusted for multiple testing. See Supplementary Tables 2, 3 and 5 for additional statistical results, including results for the subclades analysed in this study.

Data Fig. 1). In contrast, the Ophiacodontidae had a strongly negative slope, which may not have been statistically significant because of the especially small available sample size ($n = 5$). Within therapsids, Therocephalia and Anomodontia had significant negative and positive trends, respectively (Supplementary Table 1 and Extended Data Fig. 2). Biarmosuchia, Dinocephalia and Gorgonopsia had non-significant jaw length regressions (Supplementary Table 1), but for these subclades, this may be due to small sample sizes (7–12 taxa each). Within cynodonts, Cynognathia and Probainognathia both had positive regression slopes but neither had significant trends (Supplementary Table 1 and Extended Data Fig. 3).

There was a clear ‘bottleneck’ in body size near the Mammaliaformes node during the Late Triassic, with Triassic–Jurassic mammaliaforms showing less variation in body size than other synapsid groups (Fig. 1c). Further, the mammaliaform ancestral jaw length (~29 mm; Table 1) and trait optimum from the best-fitting evolutionary models (~29 mm; Table 2) were both considerably shorter than those of earlier radiations (Table 1). The mammaliaform trend towards larger body sizes with time may be driven primarily by multituberculates and eutriconodontans (Supplementary Tables 1 and 2, and Extended Data Fig. 4). The therian ancestral jaw length (~24 mm) was the shortest among the five ecological radiations. Within therians, early eutherians had a significant positive trend in body size with time. Early metatherians also showed a positive trend, but it was not significant (see Discussion, Supplementary Table 1 and Extended Data Fig. 5).

In evolutionary model-fitting analyses of body sizes (that is, \log_{10} -transformed jaw lengths), the multiple-peak Ornstein–Uhlenbeck evolutionary models (OUM) consistently received stronger support than other fitted models, including Brownian motion (BM), early burst (EB), ‘release’, and ‘release and radiate’ models (see Methods). Full results of these analyses are reported in Supplementary Table 4, and truncated results are in Table 2. The best-fitting model was a four-peak model (OUM4_Cy_Mf_Tn) with trait optima (θ) that vary among pelycosaur + therapsids, cynodonts, mammaliaforms and therians. Two additional models were similarly strong fits to the data (with Δ AICc values of -2; Table 2): a three-peak OU model (OUM3_Mf_Tn) with varying trait optima for non-mammaliaform synapsids, mammaliaforms and therians, and a five-peak model (OUM5) with trait optima for all five groups (Fig. 1d). For each of the three best-fitting models, the jaw length optima are smaller for mammaliaforms and therians than for non-mammaliaform synapsid groups (Table 2).

Diet patterns

Correlation analyses, regressions and ancestral-state reconstructions indicated that all five major radiations exhibited trends from

faunivory-only to faunivory-and-herbivory (Table 1, Figs. 1b and 2, and Extended Data Fig. 7). Pelycosaur had the weakest statistical support for this trend because the regression and correlation analyses are not significant (Table 2 and Supplementary Table 5), but the ancestral-state reconstruction for the basal node (that is, the node for Synapsida) had a faunivory likelihood of >0.999.

In addition, some less inclusive subclades also displayed this trend of greater dietary diversity with time (Supplementary Tables 1 and 2, and Extended Data Figs. 1–6). However, this pattern was not present in many of the subclades that we investigated, due in part to many of the subclades consisting entirely of faunivores (for example, Sphenacodontidae, Spalacotherioidea) or herbivores (for example, Anomodontia). Most pelycosaur and therapsid subclades showed no trend except for Therocephalia, which had a positive correlation between diet (towards greater herbivory) and patristic distance (Supplementary Table 2, and Extended Data Figs. 1 and 2). Multituberculata exhibited an omnivore-to-herbivore trend with time (Extended Data Fig. 4), consistent with previous research^{33,34}. Within Theria, early eutherians showed a strong trend towards increased dietary diversity with time, whereas our early metatherian sample showed no dietary trend with time (but see comments on metatherian results in the Discussion, Extended Data Fig. 5, and Supplementary Tables 1 and 2).

There was an especially distinct faunivory ‘bottleneck’ near the Mammaliaformes node, which is at the same phylogenetic position as the body size ‘bottleneck’ (Fig. 1b,c). Although early mammaliaforms achieved considerable dietary diversity that included carnivory and plant-dominated omnivory^{28,35–38}, many of the herbivorous mammaliaform lineages do not appear in the fossil record until the Late Cretaceous and Palaeocene^{33,34,39,40}, more than 100 Myr after mammaliaforms originated.

Discussion

We used a comprehensive ‘metatree’ of non-mammalian synapsids and a number of Mesozoic and Palaeogene mammals to investigate whether ‘small-bodied faunivore’ was the ancestral ecomorphotype for the major five major synapsid evolutionary radiations. Our results indicate faunivory is indeed the ancestral diet for the different synapsid radiations, but a small ancestral body size is a feature of only later synapsid radiations.

Radiation forerunners are faunivorous but not always small

Contrary to our expectations, we did not find universal support for the hypothesis that relatively small-bodied faunivores are the progenitors of synapsid groups that experienced major ecological radiations. Although faunivory is the typical ancestral dietary regime of each major

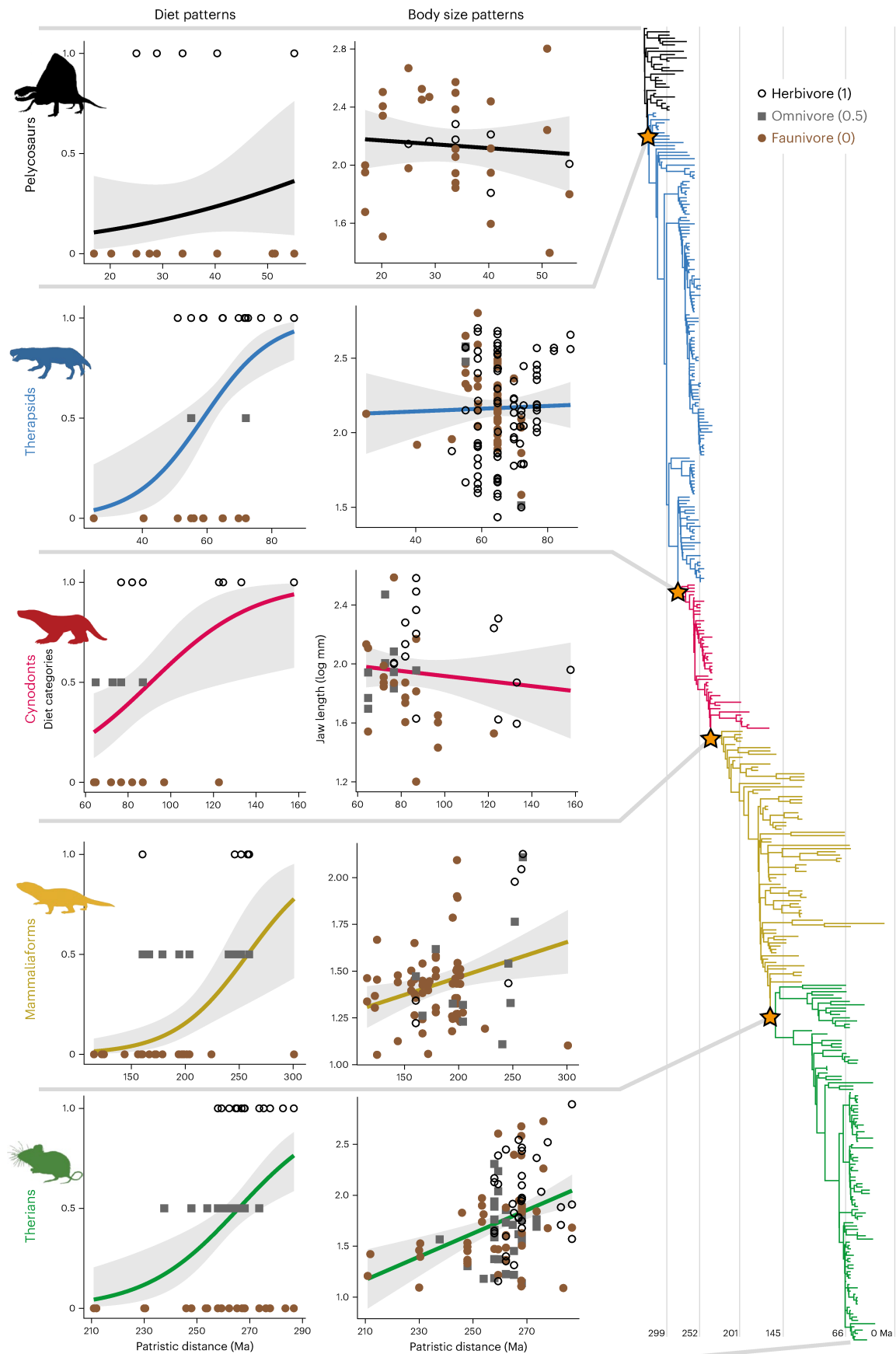


Fig. 2 | Diet and jaw length plotted against patristic distance for each of the five major synapsid radiations. Diet regressions are quasibinomial models and jaw length regressions are linear models. Grey bands are 95% confidence intervals. On the right is the dated metaphylogeny of 404 synapsid species. Stars mark the

basal phylogenetic node of each major ecological radiation. See Extended Data Figs. 1–6 for regression plots for subclades within each major radiation, and see Extended Data Figs. 1–5 and Supplementary Fig. 1 for cladograms with tip labels. See Fig. 1 caption for silhouette attribution information.

Table 2 | Summary of relative fits and parameters for evolutionary models fit to jaw length data

Evolutionary models	Summary statistics					Jaw length (mm) optima or mean				
	AICc	Δ AICc	Weight	α	σ^2	Pe	Td	Cy	Mf	Tn
BM1	197.03	197.03	0.000			(100.60)
OUI	142.11	142.11	0.000	0.028	0.010	(57.89)
EB1	199.06	199.06	0.000			(100.60)
OUM2_Td	140.45	140.45	0.000	0.031	0.010	121.94	(52.75)
OUM2_Cy	122.20	122.20	0.003	0.047	0.012	(130.52)	(41.07)
OUM2_Mf	120.31	120.31	0.009	0.049	0.012	(116.46)	(37.83)
OUM2_Tn	145.20	145.20	0.000	0.028	0.010	(58.90)	59.42
OUM3_Td_Cy	124.17	124.17	0.001	0.047	0.012	124.00	135.42	(41.07)
OUM3_Td_Mf	122.25	122.25	0.003	0.049	0.012	124.18	(112.85)	(37.83)
OUM3_Td_Tn	142.33	142.33	0.000	0.031	0.010	121.89	(51.00)	56.98
OUM3_Cy_Mf	119.01	119.01	0.016	0.052	0.012	(131.40)	74.68	(37.67)
OUM3_Cy_Tn	120.67	120.67	0.007	0.049	0.012	(130.61)	35.51		51.03
OUM3_Mf_Tn	114.25	114.25	0.178	0.056	0.013	(117.33)	29.37	50.41
OUM4_Td_Cy_Mf	120.96	120.96	0.006	0.052	0.012	124.51	136.49	74.73	37.66	
OUM4_Td_Cy_Tn	122.65	122.65	0.003	0.049	0.012	124.21	135.39	(35.52)	51.02
OUM4_Td_Mf_Tn	116.17	116.17	0.068	0.056	0.013	124.92	(113.83)	29.37	50.40
OUM4_Cy_Mf_Tn	112.14	112.14	0.509	0.061	0.013	(132.08)	75.49	29.25	50.17
OUM5	114.09	114.09	0.193	0.061	0.013	125.36	136.89	75.53	29.24	50.17

Fitted models include a single-regime Ornstein–Uhlenbeck model (OUI), single-regime BM, EB and multiple-peak OUM models. See Supplementary Table 4 for full model-fitting results, which include additional ‘shift’ models that are not reported here. Numbers after ‘OUM’ in the model names represent the number of regimes (that is, ‘peaks’), and abbreviated clade names represent the nodes that differentiate model regimes. Model parameters include the strength of attraction to trait optima (α), evolutionary step rate (σ^2) and trait optima (θ). ‘Weight’ is the Akaike weight. Parentheses in the table define the groups that are included in each model regime. For example, for the OUM2_Cy model, the two regimes are (1) ‘pelycosaurs’ + ‘therapsids’ and (2) all other taxa (that is, Cynodontia). We used \log_{10} -transformed jaw lengths for analyses, but we back-transformed the length optima here for ease of interpretation. The three best-fitting models are in bold. Cy, cynodonts; Mf, mammaliaforms; Pe, pelycosaurs; Td, therapsids; Tn, therians.

ecological radiation, the radiation forerunners are not always small in size; the tendency for ancestral taxa of radiations to be relatively small bodied does not become common until the end-Triassic size bottleneck near the base of Mammaliaformes (Figs. 1 and 2, Table 2 and Supplementary Tables 1–3). Furthermore, mammaliaforms do not show an especially strong trend towards greater body size diversity with time; their correlation analyses and PGLS regression are not significant (Table 1 and Supplementary Table 5), the range of body sizes among descendant lineages is suppressed compared with other groups, and the reconstructed ancestral jaw length is longer than the median value for the group (Table 1 and Supplementary Table 3). Thus, Theria is the only major radiation to show strong evidence of ancestral lineages being relatively small-bodied compared with descendant lineages.

In previous non-mammaliaform synapsid radiations, some subclades show statistically significant trends in body size evolution, but those trends at smaller phylogenetic scales tend to contradict each other, resulting in no overall trend within the higher-level radiations (Extended Data Figs. 1–6). Therapsids exemplify this: two subclades, anomodonts and therocephalians, display opposite trends (Extended Data Fig. 2). Anomodonts experience a significant trend towards larger body sizes, possibly reflecting the metabolic benefits larger body sizes would have provided given their herbivorous diet⁴¹, in addition to the clade’s re-diversification following the Permo-Triassic extinction primarily consisting of medium to large-sized taxa⁴². The opposite body size trend is seen in therocephalians. A few large-bodied species are present in the Triassic, but the overall trend towards smaller body sizes in therocephalians may reflect the impacts of the end-Guadalupian mass extinction^{43,44}.

All five major groups and many subclades showed evolutionary trends of ancestral faunivores giving rise to greater dietary diversity with time (Figs. 1 and 2, Table 2, and Supplementary Tables 1 and 2). This

pattern was supported by the ancestral-state reconstructions; all nodes of the ‘backbone’ of the synapsid phylogeny (from pelycosaurs to early therians) were reconstructed as faunivorous (Extended Data Fig. 7), indicating that faunivores consistently gave rise to groups with greater dietary diversity. Further, this result indicates that even if we had chosen additional nodes of interest for analyses, we would have maintained the same conclusion that radiation forerunners were faunivorous. One unexpected exception to the faunivore-to-herbivore trend is Metatheria, which showed no dietary trend with time (Extended Data Fig. 5, and Supplementary Tables 1 and 2). However, the earliest metatherians are thought to be mostly faunivorous⁴, and metatherian herbivores and omnivores that arise later in the Cretaceous and early Cenozoic (for example, Glasbiidae and Polydolopimorphia) are not adequately sampled in our study because these taxa are mostly known from teeth and not jaws (for example, *Glasbius*)⁴⁵. Therefore, we posit that a larger sample of early metatherians (especially those from the Cenozoic) would demonstrate the faunivory-only to faunivory-and-herbivory pattern that is common in other synapsid clades.

Body size bottleneck in early mammaliaforms

A small-body-size bottleneck in early mammaliaforms is evident from the plot of jaw lengths through time (Fig. 1c), and this is supported by the mammaliaform regressions (Fig. 2c), ancestral-state reconstructions (Table 1) and evolutionary model-fitting analyses (Fig. 1d) that all suggest very small sizes for early mammaliaforms. The positive trend with size was not as strong in mammaliaforms as it was in therians (Fig. 1c and Table 1), and the correlation analyses did not show a significant correlation between size and patristic distance in mammaliaforms, indicating a period of reduced body size diversification in the Late Triassic and Early Jurassic. All three of the best-fitting models (OUM3_Mf_Tn, OUM4_Cy_Mf_Tn, OUM5) include large shifts in trait optima in

mammaliaforms (to a much shorter jaw length) and therians (to a longer jaw length) (Fig. 1d and Table 2). Thus, each model captures both the body size bottleneck near the base of Mammaliaformes and the subsequent body size diversification of therians. The four-peak and five-peak models also describe the shift in body size evolution from pelycosaurs and therapsids to cynodonts. With a few exceptions (for example, *Cynognathus*, *Exaeretodon*, *Impidens*, *Scalenodontoides*)⁴⁶, the range of body sizes within cynodonts is more constrained to medium and small sizes (jaw length <135 mm) relative to the sizes of pelycosaurs and therapsids, which is consistent with previous findings⁴⁷. This may suggest selection against larger cynodont body sizes, or an inability of cynodonts (and early mammaliaforms) to invade ecological niches that require or accommodate larger body sizes due to the increasing ecological dominance of diapsid reptiles in the Triassic.

The appearance of very small body sizes is one of several aspects of the mammalian phenotype to emerge in the Late Triassic and Early Jurassic. Other traits include a determinate pattern of skull growth, the novel dentary-squamosal jaw joint, smaller ‘post-dentary’ bones free from functional constraints associated with mastication, a more ossified braincase and orbital wall, diphodont tooth replacement, mammal-like regionalization of the vertebral column and endothermy^{48–59}. We follow previous studies in positing that small body size may have been a prerequisite or catalyst for the evolution of some of these traits. For example, ref. 60 argued that especially small body size may have helped facilitate the evolutionary transition of jaw joint bones (quadrate, articular) to the middle ear (incus, malleus) by reducing biomechanical stresses at the jaw joint. Further, the evolution of endothermy in mammalian ancestors has been linked to the shift to smaller body size^{59,61,62}.

Many mammaliaforms and therians were already at or near their absolute minimum body size during the Jurassic and Cretaceous, the lower bound of which is probably determined by physiological or metabolic constraints^{41,63}. The absolute minimum body size for mammals may act as an evolutionary ‘reflecting boundary’ (sensu ref. 64) such that larger body size was the only available morphological space into which mammaliaforms and therians could evolve⁶⁵. Therefore, the trends towards larger body size in mammaliaforms and therians may reflect passive trends away from small body size rather than active trends towards larger size⁶⁴ (but see refs. 29,65 for an opposing view). Mammaliaforms and early therians may have been restricted to small body sizes during the Mesozoic because of competition with or predation by the dominant dinosaur fauna^{37,66–69} (but for alternative views, see refs. 4,33,70,71). Once niche space opened up after faunal turnover events of the Cretaceous Terrestrial Revolution (KTR)^{34,72} and the Cretaceous–Palaeogene (K–Pg) mass extinction (for example, ref. 45), mammalian body size diversification may have trended (passively or actively) towards larger sizes^{27,28,67–69,73}. In this way, the end-Triassic body size bottleneck permanently altered macroevolutionary dynamics for the remainder of synapsid history, although this change did not fully manifest itself until after the KTR and/or K–Pg extinction, over 100 Myr later.

Survival of the relatively novel faunivores

As a potential causal mechanism for the observed macroevolutionary pattern that faunivores are the forerunners of major radiations, it is tempting to turn to Cope’s ‘law of the unspecialized’^{6,717–22,31}. This ‘law’ states that ecologically unspecialized species have a reduced risk of extinction compared with highly specialized species; thus, unspecialized taxa are more likely to survive extinction events and subsequently radiate. Hypothetically, if most faunivores (or at least insectivores) are considered less ecologically specialized than herbivores, then faunivorous lineages may be more likely to experience long-term survival and give rise to subsequent radiations (as we observe here), whereas herbivorous clades have a greater risk of extinction^{20,74}. ‘Survival of the relatively unspecialized’ has been used to help explain the mammalian

trend towards larger body sizes with time (as seen in our mammaliaform and therian results)^{7,21}, which is often attributed to Cope’s rule²⁹.

However, we do not consider ‘survival of the unspecialized’ to fully explain our results, for at least two reasons. First, ‘survival of the unspecialized’ refers to being ecologically unspecialized, and although ‘omnivore’ is often considered the most generalized dietary group, we did not find evidence of omnivory being the ancestral dietary regime of major radiations. Second, although many of the progenitors of major synapsid radiations may appear to be morphologically unspecialized faunivores, this does not mean that they are ecologically unspecialized. For instance, recent studies have shown that early insectivorous mammaliaforms exhibited greater niche partitioning than previously assumed^{75,76}.

Further, the view that early lineages of radiations are morphologically (or ecologically) unspecialized might simply be due to observational bias: the early lineages of each radiation are morphologically ‘unspecialized’ relative to many of their later descendant lineages, but they also can be very derived compared with their contemporaries. For instance, early therians were small-bodied insectivores or omnivores that are relatively unspecialized compared with descendant clades, which include extant mammals (besides monotremes) that have achieved extreme levels of ecomorphological diversity. Relative to contemporary clades in the Mesozoic Era, however, therians could be considered very derived and morphologically specialized. For example, they (or their close relatives) evolved a tribosphenic molar that permitted more complex masticatory functions than most coeval faunivores^{77,78}, novel masticatory movements via asynchronous contractions of jaw muscles^{79–82}, and improved auditory and olfactory senses via evolutionary changes to the cochlea⁵⁸ and face⁸³, respectively. A similar pattern applies to the other synapsid radiations, with as many as 55 novel synapomorphies differentiating early therapsids from pelycosaurs^{84,85} and 27 synapomorphies separating cynodonts from other therapsids⁸⁶. Thus, rather than ‘survival of the unspecialized’, we argue that our results support the ‘survival of the relatively novel’⁸⁷.

Many of these novel traits, which could be considered ‘key innovations’, may have played a larger role in survival than diversification. The origins of these traits (and the clades that possess the traits) rarely coincide with the start of evolutionary radiations, indicating that the traits themselves did not catalyse the radiations. For instance, therians (or closely related taxa) with novel molar, ear and facial traits experienced a macroevolutionary lag⁸⁸: they evolved by the Middle Jurassic (~165 Ma)⁸⁹ but did not begin to ecologically radiate until the middle or Late Cretaceous, ~75 Myr after their origin^{4,37,70}. Rather than catalysing radiations, the novel traits may have facilitated long-term lineage survival during mass extinctions and other faunal turnover events. Therapsids evolved by the late Pennsylvanian, but their diversification is only recorded in the middle Permian, following Olson’s extinction, and the main cynodont radiation occurs in the aftermath of the Permo-Triassic mass extinction despite the clade’s origin in the middle Permian^{23,90–97}. Similarly, early mammaliaforms survived the Triassic–Jurassic mass extinction, and therians survived the KTR and K–Pg mass extinction²⁸. In each case, the opening of ecological niche space through the removal of previous incumbents seems to be the key step in beginning the subsequent diversification^{34,71}. This pattern is consistent with evidence from early amniotes, including the first synapsids, which demonstrates that extinction predates the start of evolutionary radiations at that stage of tetrapod evolution as well⁸⁷.

Conclusions

Using a new time-calibrated metatree of fossil synapsids spanning ~300 Myr, we rigorously tested hypotheses of body size and diet evolution. Specifically, we asked whether the early members of synapsid evolutionary radiations consisted of relatively small-bodied faunivores, with later members exhibiting a broader range of diets and a trend towards larger body sizes. We found that faunivory is the typical

ancestral dietary regime of each major radiation within Synapsida, but the small-to-large trend in body size within radiations does not become common until the end-Triassic size bottleneck near the base of Mammaliaformes. Our results indicate a shift to smaller ancestral sizes at the base of Cynodontia, with stronger shifts at the base of Mammaliaformes and Theria. In turn, these changes caused subsequent radiations to exhibit small-to-large trends in size evolution, although these trends may be passive due to the ancestral sizes being close to the lower limit possible for the clades. The Triassic shift to small ancestral body sizes altered synapsid macroevolutionary dynamics, although this change was not fully realized until the Cenozoic diversification of therian mammals. Finally, although the progenitors of synapsid radiations appear relatively unspecialized in hindsight, they typically possess important novel characters compared with their contemporaries. These characters were likely important in promoting their long-term survival and diversification (that is, 'survival of relatively novel faunivores'), but it appears that mass extinctions and other faunal turnovers were necessary for the lineages that possessed these characters to reach their full evolutionary potential. The past decade has witnessed a resurgence of research on non-mammaliaform synapsids, and our new comprehensive metaphylogeny provides a rigorous foundation for continuing work on macroevolutionary patterns and processes among the forerunners of mammals.

Methods

Metatree

To examine synapsid macroevolutionary patterns in a phylogenetic context, we built a metatree of 2,130 synapsid species. Our time-calibrated metatree contains 1,888 species from the Carboniferous through the Eocene (305–34 Ma). We follow the metatree approach described in refs. 32,98, using the metatree⁹⁸ (<https://github.com/graelmetilloyd/metatree>) and Claddis⁹⁹ packages in R¹⁰⁰, as well as the maximum parsimony software TNT v.1.1 (ref. 101). For non-mammaliaform synapsids, we collected every morphological character matrix that has ever been published (to the best of our knowledge) as of July 2021, in which non-mammaliaform synapsids composed the majority of the operational taxonomic units (OTUs). We also collected the most comprehensive early mammaliaform character matrices. We collected 269 matrices in total from 241 source studies (Supplementary Table 6). Due to evolving ideas of relationships and frequent matrix reuse, each of the matrices was weighted according to its publication year and its dependence on 'parent' matrices using an established procedure (Supplementary Methods)^{32,98}.

For the non-therian radiations, our aim was to capture macroevolutionary patterns over the entire evolutionary duration of the group. However, examining macroevolutionary patterns for all of Theria is beyond the scope of this study, as it would require intense sampling of the incredibly numerous later Cenozoic taxa (for example, ref. 102 identified 6,495 extant and recently extinct mammalian species and this excludes the vast majority of Cenozoic fossil mammals). Instead, for Theria our aim was to examine the first ~100 Myr of evolution, from the origin of the clade (~165 Ma)⁸⁹ through the evolution of many of the modern orders in the early Paleogene. Thus, our results for Theria only reflect the early history of the clade, but our sampling is sufficient to establish its ancestral body size and diet, and to determine whether there is an initial trend towards the evolution of larger size among its members. See Supplementary Methods for additional discussion on our therian sample.

The metatree approach relies on XML metadata files that reconcile OTU names to valid Paleobiology Database¹⁰³ (PBDB; www.paleobiodb.org) taxa^{32,98}. We resolved OTU names in matrices to match with taxon names in the PBDB. This was a time-consuming task that must be done carefully and deliberately. We made a total of ~400 revisions to the PBDB in the course of this project, including adding taxa, correcting mis-spellings and correcting/adding taxonomic lineage information.

Further, we deleted unnamed specimen-level OTUs and those not present in the PBDB. Many OTUs in character matrices are only given at the genus level, but our metatree is at the species level. In these cases, we examined the original publications for information on which particular species were used to score each genus and used these in the XML files.

In early metatree analyses, some relationships of early synapsid clades were especially unstable or contradictory to consensus views within the literature. This appears to result from the fact that relatively few analyses of higher-level relationships among major therapsid clades have been undertaken, but that small numbers of outgroup taxa are included in the many analyses of relationships within major clades. Most of these within-clade datasets are not designed to resolve outgroup relationships and they sometimes recover results that conflict with the few higher-level analyses that have been conducted (for example, the relatively stemward position of Gorgonopsia and the paraphyly of Dinocephalia in most derivatives of the anomodont data matrix of ref. 104). Thus, to ensure that the metatree topology reflected the current understanding of higher-level non-mammalian synapsid relationships, we used the phylogenetic tree of ref. 84 to constrain some of the higher-level relationships within the metatree.

To time calibrate the majority-rule topology, we began by querying the PBDB to obtain occurrence ages (Supplementary Table 7). We then vetted all PBDB age data, supplementing or updating them with biostratigraphic or radiometric age estimates from primary sources as much as possible. PBDB ages were revised for ~10% of sampled species. For Cretaceous and early Palaeocene therian age ranges, we relied primarily on previously reported ages⁴. Reliable occurrence data were obtained for 1,888 of the taxa in the phylogeny. After dropping the taxa for which we did not have occurrence data, we used the timePaleoPhy function within the paleotree R package¹⁰⁵ to date the metatree. Although we later dropped tips representing taxa for which jaw length measurements were not available, these were included during the time-scaling process because they provided important branch length and node age information¹⁰⁶.

The strict consensus topology of our metatree contained large polytomies within Mammaliaformes. To circumvent this issue, we used the majority-rule topology (see Supplementary Fig. 1 for our analyses).

We divided synapsids into five ecological radiations, which are well established in the literature as distinct major radiations^{23,26–28}. See Supplementary Methods for a detailed description of these radiations, including discussion of their derived morphological traits and evidence that they have each undergone ecological diversification. Further, the Supplementary Methods includes discussion on some clades with controversial topological positions (for example, varanopids, allotherians). For supplementary analyses, we divided the five major radiations into 19 subclades and results for these groups are provided in Supplementary Results. Finally, we repeated some analyses using Mammalia to help test whether our choice of clades influenced results (Supplementary Tables 1–3).

Body size proxies and dietary classification

We used jaw length as a proxy for body size, in part because many different measurements have been used to approximate body size in different groups of synapsids^{20,33,47}, making it challenging to produce consistent estimates across all synapsid groups. Further, jaws are commonly preserved in the synapsid fossil record, thus providing us with a large sample size. We collected jaw length measurements and dietary information for 404 synapsid species (37 pelycosaurs, 134 therapsids, 45 cynodonts, 78 mammaliaforms and 110 therians). Jaws were measured from photographs taken by the authors and published figures in the literature (Supplementary Table 7). In cases where we had more than one measurement for a species, we used the longest jaw length to help minimize the chance of including juveniles in our sample. Jaw lengths were measured as the distance from the anterior tip of the dentary to the jaw joint/posterior condylar process, parallel to the cheek teeth row

(sensu ref. 16). For mammaliaforms and mammals without preserved anterior portions of the jaw, we used a regression equation based on data from extant mammals¹⁶ to estimate jaw lengths from the distance between the first lower molar and jaw joint (see Supplementary Methods). Jaw lengths were \log_{10} -transformed before analyses.

Dietary information was taken from the PBDB and vetted using information from the scientific literature and inferences from dental morphologies, resulting in several species' diets that were altered from the PBDB classifications (Supplementary Table 7). We grouped taxa into one of three diet categories: faunivores, omnivores or herbivores. Insectivores, carnivores and piscivores were included in the faunivore category. Although these three categories are an oversimplification of the dietary diversity in the mammalian lineage, we could not use more specific diet categories because detailed dietary information is unavailable for many early synapsid groups. Further, many of the food items of extant mammals (for example, grasses and fleshy fruits) were not present for much of synapsid history, hence narrower diet categories (for example, 'grazing herbivore' or 'frugivore') might not be applicable to a majority of our sample. See Supplementary Methods for additional discussion.

To quantify diets for some analyses, we assigned a number to each of the three diet categories: 0, faunivores; 0.5, omnivores; and 1, herbivores. We chose these values because they represent approximations of the percentages of plant material in each of the diets (for example, many herbivores have diets consisting of 100% plants), thus allowing us to treat the diets as proportional data in regression analyses.

Regression and correlation analyses

We used two types of analyses to quantify trends in body size and diet across the five major synapsid groups (Supplementary Methods) and their subclades. First, we examined the relationship between jaw lengths and patristic distance using linear models, and we examined the relationship between diet and patristic distance using quasibinomial generalized linear models, which can be fit to proportional data. We used OLS regressions for our primary linear model results (Table 1), but we also performed supplementary regression analyses via PGLS (Supplementary Table 5). PGLS regressions were performed using the `gls` function of the `nlme` R package¹⁰⁷, with phylogenetic signal (Pagel's λ) incorporated into analyses and calculated via maximum likelihood. Because omnivores and herbivores were assigned larger values (0.5 and 1, respectively) than faunivores (0), for diet regressions, a positive relationship indicates an increased number of omnivorous and/or herbivorous lineages with time. Patristic distance provides a measure of the phylogenetic proximity of each taxon to a selected node within a phylogeny¹⁰⁸, and comparisons between morphology and patristic distance have been used in previous studies of trends in synapsid evolution^{48,49,109,110}. We calculated patristic distance as the sum of branch lengths in units of time from each taxon in our sample to our outgroup taxon, the oldest known sauropsid *Hylonomus lyelli*¹¹¹.

Second, we tested for a correlation between our data (jaw lengths or diets) and patristic distances using both the Kendall rank correlation coefficient and the Spearman rank correlation coefficient. Our quantitative dietary categories (0, 0.5 and 1) are arbitrarily ranked values, hence correlation analyses may be more statistically appropriate than regressions. We used the `cor.test` R function with the setting 'exact = FALSE' due to some identical paired values among diet data (that is, species with the same patristic distance and diet) and because some sample sizes among subclades were less than 50. Results for Kendall rank and Spearman rank were very similar (Table 1 and Supplementary Table 2).

Evolutionary model-fitting analyses

We fit 44 evolutionary models to the jaw length data (\log_{10} mm) using the `mvMORPH` R package¹¹², following the methods in ref. 106. We fit three categories of models: (1) 'uniform' models that treat all taxa as a single selective regime, (2) 'shift' models that allow for a single shift

in mode of evolution at a specific node and (3) multiple-regime (or multiple-peak) Ornstein–Uhlenbeck (OU) models¹¹³ that test for a shift in trait optima at one or more nodes. Uniform models included BM ('random walk'), OU and EB models. Shift models included the 'radiate' (OU shifting to BM with a constant evolutionary rate) and 'release and radiate' (OU shifting to BM with a shift in rate) models⁶⁹, as well as variations of the 'release' and 'release and radiate' models in which BM shifts to OU. We also tested for BM evolution with rate shifts (that is, BMM models)¹¹². We tested for shifts at five nodes: Therapsida, Cynodontia, Mammaliaformes, Mammalia and Theria. Mammalia is not one of the major radiations that we focus on in this study, but we included it to test whether a more significant shift occurred at the mammalian node than at the mammaliaform or therian nodes. Multiple OUM models were fit to the data using various combinations of nodes. For instance, the `OUM3_Cy_Mf` model is a three-regime model that allows for shifts in trait optima at the Cynodontia (Cy) and Mammaliaformes (Mf) nodes (that is, the three regimes are non-cynodont synapsids, non-mammaliaform cynodonts and mammaliaforms). For OUM models, we assumed the oldest regime state to be stationary (that is, the 'root' parameter was set to 'FALSE') because our sample did not include non-synapsid fossil data that would inform whether there was an optimum shift at Synapsida. Model support was determined using small-sample-size-corrected Akaike Information Criterion (AICc) values¹¹⁴. In Table 2, we only report results for the OUM models and uniform models for comparison because none of the 'shift' models had AICc values within -25 of the best-fitting model (full results for all models are provided in Supplementary Table 4).

With the OUM models, trait optima are the only parameters that can vary; evolutionary rates (σ^2) and selection strength (α) are constant across regimes. It would be reasonable to expect some shifts in evolutionary rates or selection strength at different nodes, and shifts in rate and selection strength should be explored in future work.

Ancestral-state reconstructions

To understand the degree and direction of body size evolution in more detail, we calculated the ancestral jaw length of each major radiation with the `reconstruct` function in the R package `ape`¹¹⁵. This function uses maximum likelihood and assumes a BM mode of evolution across the full phylogeny. Because some groups are unlikely to have evolved via BM (for example, see our evolutionary model-fitting results), we performed additional ancestral reconstructions for jaw lengths after first testing whether single-regime BM or OU models were better fits to the data for individual radiations (the phylogeny was pruned to include only the taxa of that radiation). Models were fit using the `mvMORPH` R package¹¹². We calculated ancestral jaw lengths for each radiating group using the best-fitting model. We report and discuss the results in Supplementary Table 5 and the Supplementary Results, respectively.

We calculated ancestral states for discrete diets (faunivore, omnivore, herbivore) using the `ace` function in the `ape` R package. We used the default 'REML' method and assumed equal transition rates among diets.

Reporting summary

Further information on research design is available in the Nature Portfolio Reporting Summary linked to this article.

Data availability

All data used in this study are available through the main tables and the Supplementary Information.

Code availability

A simplified version of the R code used for this study is available as a supplementary text file. The code used to create the metatree is available at <https://github.com/graemetlloyd/metatree>.

References

- Rabosky, D. L. & Lovette, I. J. Explosive evolutionary radiations: decreasing speciation or increasing extinction through time? *Evolution* **62**, 1866–1875 (2008).
- Alfaro, M. E. et al. Nine exceptional radiations plus high turnover explain species diversity in jawed vertebrates. *Proc. Natl Acad. Sci. USA* **106**, 13410–13414 (2009).
- O’Leary, M. A. et al. The placental mammal ancestor and the post-K–Pg radiation of placentals. *Science* **339**, 662–667 (2013).
- Grossnickle, D. M. & Newham, E. Therian mammals experience an ecomorphological radiation during the Late Cretaceous and selective extinction at the K–Pg boundary. *Proc. R. Soc. B* **283**, 20160256 (2016).
- Bouchenak-Khelladi, Y., Onstein, R. E., Xing, Y., Schwery, O. & Linder, H. P. On the complexity of triggering evolutionary radiations. *New Phytol.* **207**, 313–326 (2015).
- Cope, E. D. *The Primary Factors of Organic Evolution* (Open Court Publishing, 1896).
- Stanley, S. M. An explanation for Cope’s rule. *Evolution* **27**, 1–26 (1973).
- Pough, F. H. Lizard energetics and diet. *Ecology* **54**, 837–844 (1973).
- Gaulin, S. J. A Jarman/Bell model of primate feeding niches. *Hum. Ecol.* **7**, 1–20 (1979).
- Tomiya, S. Body size and extinction risk in terrestrial mammals above the species level. *Am. Nat.* **182**, E196–E214 (2013).
- Zanno, L. E. & Makovicky, P. J. No evidence for directional evolution of body mass in herbivorous theropod dinosaurs. *Proc. R. Soc. Lond. B* **280**, 20122526 (2013).
- Reisz, R. R. & Fröbisch, J. The oldest caseid synapsid from the Late Pennsylvanian of Kansas, and the evolution of herbivory in terrestrial vertebrates. *PLoS ONE* **9**, e94518 (2014).
- Price, S. A. & Hopkins, S. S. The macroevolutionary relationship between diet and body mass across mammals. *Biol. J. Linn. Soc.* **115**, 173–184 (2015).
- Pineda-Munoz, S., Evans, A. R. & Alroy, J. The relationship between diet and body mass in terrestrial mammals. *Paleobiology* **42**, 659–669 (2016).
- Brocklehurst, N. & Brink, K. S. Selection towards larger body size in both herbivorous and carnivorous synapsids during the Carboniferous. *FACETS* **2**, 68–84 (2017).
- Grossnickle, D. M. Feeding ecology has a stronger evolutionary influence on functional morphology than on body mass in mammals. *Evolution* **74**, 610–628 (2020).
- Simpson, G. G. *Tempo and Mode in Evolution* (Columbia Univ. Press, 1944).
- Liow, L. H. A test of Simpson’s “Rule of the Survival of the Relatively Unspecialized” using fossil crinoids. *Am. Nat.* **164**, 431–443 (2004).
- Liow, L. H. Lineages with long durations are old and morphologically average: an analysis using multiple datasets. *Evolution* **61**, 885–901 (2007).
- Smits, P. D. Expected time-invariant effects of biological traits on mammal species duration. *Proc. Natl Acad. Sci. USA* **112**, 13015–13020 (2015).
- Raia, P. & Fortelius, M. Cope’s law of the unspecialized, Cope’s rule, and weak directionality in evolution. *Evol. Ecol. Res.* **15**, 747–756 (2013).
- Raia, P. et al. Progress to extinction: increased specialisation causes the demise of animal clades. *Sci. Rep.* **6**, 30965 (2016).
- Angielczyk, K. D. & Kammerer, C. F. in *Handbook of Zoology: Mammalia: Mammalian Evolution, Diversity and Systematics* (eds Zacos, F. E. & Asher, R. J.) 117–198 (De Gruyter, 2018).
- Osborn, H. F. The law of adaptive radiation. *Am. Nat.* **36**, 353–363 (1902).
- Broom, R. 1932. *The Mammal-like Reptiles of South Africa and the Origin of Mammals* (H. F. & G. Witherby, 1932).
- Hopson, J. A. The origin and adaptive radiation of mammal-like reptiles and nontherian mammals. *Ann. N. Y. Acad. Sci.* **167**, 199–216 (1969).
- Kemp, T. S. *The Origin and Evolution of Mammals* (Oxford Univ. Press, 2005).
- Grossnickle, D. M., Smith, S. M. & Wilson, G. P. Untangling the multiple ecological radiations of early mammals. *Trends Ecol. Evol.* **34**, 936–949 (2019).
- Alroy, J. Cope’s rule and the dynamics of body mass evolution in North American fossil mammals. *Science* **280**, 731–734 (1998).
- Raia, P., Carotenuto, F., Passaro, F., Fulgione, D. & Fortelius, M. Ecological specialization in fossil mammals explains Cope’s rule. *Am. Nat.* **179**, 328–337 (2012).
- Polly, P. D. Cope’s rule. *Science* **282**, 50–52 (1998).
- Lloyd, G. T. et al. Probabilistic divergence time estimation without branch lengths: dating the origins of dinosaurs, avian flight, and crown birds. *Biol. Lett.* **12**, 20160609 (2016).
- Wilson, G. P. et al. Adaptive radiation of multituberculate mammals before the extinction of dinosaurs. *Nature* **483**, 457–460 (2012).
- Grossnickle, D. M. & Polly, P. D. Mammal disparity decreases during the Cretaceous angiosperm radiation. *Proc. R. Soc. Lond. B* **280**, 20132110 (2013).
- Hu, Y., Meng, J., Wang, Y. & Li, C. Large Mesozoic mammals fed on young dinosaurs. *Nature* **433**, 149–152 (2005).
- Luo, Z.-X. et al. New evidence for mammaliaform ear evolution and feeding adaptation in a Jurassic ecosystem. *Nature* **548**, 326–329 (2017).
- Chen, M., Strömberg, C. A. & Wilson, G. P. Assembly of modern mammal community structure driven by Late Cretaceous dental evolution, rise of flowering plants, and dinosaur demise. *Proc. Natl Acad. Sci. USA* **116**, 9931–9940 (2019).
- Morales-García, N. M., Gill, P. G., Janis, C. M. & Rayfield, E. J. Jaw shape and mechanical advantage are indicative of diet in Mesozoic mammals. *Commun. Biol.* **4**, 242 (2021).
- Krause, D. W. et al. First cranial remains of a gondwanatherian mammal reveal remarkable mosaicism. *Nature* **515**, 512–517 (2014).
- Harper, T., Parras, A. & Rougier, G. W. *Reigitherium* (Meridiolestida, Mesungulatoidea) an enigmatic Late Cretaceous mammal from Patagonia, Argentina: morphology, affinities, and dental evolution. *J. Mamm. Evol.* **26**, 447–478 (2019).
- Peters, R. H. *The Ecological Implications of Body Size* (Cambridge Univ. Press, 1986).
- Angielczyk, K. D. & Walsh, M. L. Patterns in the evolution of nares size and secondary palate length in anomodont therapsids (Synapsida): implications for hypoxia as a cause of end-Permian tetrapod extinctions. *J. Paleontol.* **82**, 528–542 (2008).
- Huttenlocker, A. K. Body size reductions in nonmammalian eutheriodont therapsids (Synapsida) during the end-Permian mass extinction. *PLoS ONE* **9**, e87553 (2014).
- Grunert, H. R., Brocklehurst, N. & Fröbisch, J. Diversity and disparity of Therocephalia: macroevolutionary patterns through two mass extinctions. *Sci. Rep.* **9**, 5063 (2019).
- Wilson, G. P. Mammals across the K/Pg boundary in northeastern Montana, USA: dental morphology and body-size patterns reveal extinction selectivity and immigrant-fueled ecospace filling. *Paleobiology* **39**, 429–469 (2013).
- Tolchard, F. et al. A new large gomphodont from the Triassic of South Africa and its implications for Gondwanan biostratigraphy. *J. Vertebr. Paleontol.* **41**, e1929265 (2021).
- Sookias, R. B., Butler, R. J. & Benson, R. B. J. Rise of dinosaurs reveals major body-size transitions are driven by passive processes of trait evolution. *Proc. R. Soc. Lond. B* **279**, 2180–2187 (2012).

48. Sidor, C. A. Simplification as a trend in synapsid cranial evolution. *Evolution* **55**, 1419–1442 (2001).
49. Sidor, C. A. Evolutionary trends and the origin of the mammalian lower jaw. *Paleobiology* **29**, 605–640 (2003).
50. Kielan-Jaworowska, Z., Cifelli, R. L. & Luo, Z.-X. *Mammals from the Age of Dinosaurs: Origins, Evolution, and Structure* (Columbia Univ. Press, 2004).
51. Rowe, T. B., Macrini, T. E. & Luo, Z.-X. Fossil evidence on origin of the mammalian brain. *Science* **332**, 955–957 (2011).
52. Benoit, J., Abdala, F., Manger, P. R. & Rubidge, B. S. The sixth sense in mammalian forerunners: variability of the parietal foramen and the evolution of the pineal eye in South African Permo-Triassic eutheriodont therapsids. *Acta Palaeontol. Pol.* **61**, 777–789 (2016).
53. Rey, K. et al. Oxygen isotopes suggest elevated thermometabolism within multiple Permo-Triassic therapsid clades. *eLife* **6**, e28589 (2017).
54. Guignard, M. L., Martinelli, A. G. & Soares, M. B. Reassessment of the postcranial anatomy of *Prozostrodon brasiliensis* and implications for postural evolution of non-mammaliaform cynodonts. *J. Vertebr. Paleontol.* **38**, e1511570 (2018).
55. Guignard, M. L., Martinelli, A. G. & Soares, M. B. The postcranial anatomy of *Brasilodon quadrangularis* and the acquisition of mammaliaform traits among non-mammaliaform cynodonts. *PLoS ONE* **14**, e0216672 (2019).
56. Benoit, J. et al. The evolution of the maxillary canal in Probainognathia (Cynodontia, Synapsida): reassessment of the homology of the infraorbital foramen in mammalian ancestors. *J. Mamm. Evol.* **27**, 329–348 (2020).
57. Jones, K. E., Gonzalez, S., Angielczyk, K. D. & Pierce, S. E. Regionalization of the axial skeleton predates functional adaptation in the forerunners of mammals. *Nat. Ecol. Evol.* **4**, 470–478 (2020).
58. Luo, Z.-X. & Manley, G. A. in *The Senses: A Comprehensive Reference* Vol. 2 (eds Fritzsche, B. & Grothe, B.) 207–252 (Elsevier Academic Press, 2020).
59. Araujo, R. et al. Inner ear biomechanics reveals a Late Triassic origin for mammalian endothermy. *Nature* **607**, 726–731 (2022).
60. Lautenschlager, S. et al. The role of miniaturization in the evolution of the mammalian jaw and middle ear. *Nature* **561**, 533–537 (2018).
61. Hopson, J. A. Endothermy, small size, and the origin of mammalian reproduction. *Am. Nat.* **107**, 446–452 (1973).
62. McNab, B. K. The evolution of endothermy in the phylogeny of mammals. *Am. Nat.* **112**, 1–21 (1978).
63. West, G. B., Woodruff, W. H. & Brown, J. H. Allometric scaling of metabolic rate from molecules and mitochondria to cells and mammals. *Proc. Natl Acad. Sci. USA* **99**, 2473–2478 (2002).
64. McShea, D. W. Mechanisms of large-scale evolutionary trends. *Evolution* **48**, 1747–1763 (1994).
65. Alroy, J. Understanding the dynamics of trends within evolving lineages. *Paleobiology* **26**, 319–329 (2000).
66. Lillegraven, J. A., Kielan-Jaworowska, Z. & Clemens, W. A. *Mesozoic Mammals: The First Two-thirds of Mammalian History* (Univ. of California Press, 1979).
67. Alroy, J. The fossil record of North American mammals: evidence for a Paleocene evolutionary radiation. *Syst. Biol.* **48**, 107–118 (1999).
68. Smith, F. A. et al. The evolution of maximum body size of terrestrial mammals. *Science* **330**, 1216–1219 (2010).
69. Slater, G. J. Phylogenetic evidence for a shift in the mode of mammalian body size evolution at the Cretaceous-Palaeogene boundary. *Methods Ecol. Evol.* **4**, 734–744 (2013).
70. Clausen, A. & Redner, S. Evolutionary model of species body mass diversification. *Phys. Rev. Lett.* **102**, 038103 (2009).
71. Brocklehurst, N., Panciroli, E., Benevento, G. L. & Benson, R. B. Mammaliaform extinctions as a driver of the morphological radiation of Cenozoic mammals. *Curr. Biol.* **31**, 2955–2963 (2021).
72. Lloyd, G. T. et al. Dinosaurs and the Cretaceous terrestrial revolution. *Proc. R. Soc. Lond. B* **275**, 2483–2490 (2008).
73. Lyson, T. R. et al. Exceptional continental record of biotic recovery after the Cretaceous–Paleogene mass extinction. *Science* **366**, 977–983 (2019).
74. Weaver, L. N. & Wilson, G. P. Shape disparity in the blade-like premolars of multituberculate mammals: functional constraints and the evolution of herbivory. *J. Mammal.* **102**, 967–985 (2021).
75. Gill, P. G. et al. Dietary specializations and diversity in feeding ecology of the earliest stem mammals. *Nature* **512**, 303–305 (2014).
76. Conith, A. J., Imburgia, M. J., Crosby, A. J. & Dumont, E. R. The functional significance of morphological changes in the dentitions of early mammals. *J. R. Soc. Interface* **13**, 20160713 (2016).
77. Schultz, J. A. & Martin, T. Function of pretribosphenic and tribosphenic mammalian molars inferred from 3D animation. *Naturwissenschaften* **101**, 771–781 (2014).
78. Jäger, K. R., Cifelli, R. L. & Martin, T. Molar occlusion and jaw roll in early crown mammals. *Sci. Rep.* **10**, 22378 (2020).
79. Williams, S. H. et al. A preliminary analysis of correlated evolution in mammalian chewing motor patterns. *Integr. Comp. Biol.* **51**, 247–259 (2011).
80. Grossnickle, D. M. The evolutionary origin of jaw yaw in mammals. *Sci. Rep.* **7**, 45094 (2017).
81. Bhullar, B. A. S. et al. Rolling of the jaw is essential for mammalian chewing and tribosphenic molar function. *Nature* **566**, 528–532 (2019).
82. Grossnickle, D. M., Weaver, L. N., Jäger, K. R. & Schultz, J. A. The evolution of anteriorly directed molar occlusion in mammals. *Zool. J. Linn. Soc.* **194**, 349–365 (2022).
83. Higashiyama, H. et al. Mammalian face as an evolutionary novelty. *Proc. Natl Acad. Sci. USA* **118**, e2111876118 (2021).
84. Sidor, C. A. & Hopson, J. A. Ghost lineages and “mammalness”: assessing the temporal pattern of character acquisition in the Synapsida. *Paleobiology* **24**, 254–273 (1998).
85. Kemp, T. S. The origin and early radiation of the therapsid mammal-like reptiles: a palaeobiological hypothesis. *J. Evol. Biol.* **19**, 1231–1247 (2006).
86. Hopson, J. A. & Kitching, J. W. A probainognathian cynodont from South Africa and the phylogeny of nonmammalian cynodonts. *Bull. Mus. Comp. Zool.* **156**, 5–35 (2001).
87. Brocklehurst, N., Ruta, M., Müller, J. & Fröbisch, J. Elevated extinction rates as a trigger for diversification rate shifts: early amniotes as a case study. *Sci. Rep.* **5**, 17104 (2015).
88. Jablonski, D. Approaches to macroevolution: 1. General concepts and origin of variation. *Evol. Biol.* **44**, 427–450 (2017).
89. Luo, Z.-X. et al. A Jurassic eutherian mammal and divergence of marsupials and placentals. *Nature* **476**, 442–445 (2011).
90. Chen, Z.-Q. & Benton, M. J. The timing and pattern of biotic recovery following the end-Permian mass extinction. *Nat. Geosci.* **5**, 375–383 (2012).
91. Benton, M. J. & Newell, A. J. Impacts of global warming on Permo-Triassic terrestrial ecosystems. *Gondwana Res.* **25**, 1308–1337 (2014).
92. Benton, M. J. *When Life Nearly Died: The Greatest Mass Extinction of All Time* (Thames & Hudson, 2015).
93. Botha, J. & Smith, R. M. H. *Lystrosaurus* species composition across the Permo-Triassic boundary of South Africa. *Lethaia* **40**, 125–137 (2007).
94. Botha-Brink, J. & Abdala, F. A new cynodont record from the *Tropidostoma* Assemblage Zone of the Beaufort Group: implications for the early evolution of cynodonts in South Africa. *Palaeontol. Afr.* **43**, 1–6 (2008).

95. Abdala, F. & Ribeiro, A. M. Distribution and diversity patterns of Triassic cynodonts (Therapsida, Cynodontia) in Gondwana. *Palaeogeogr. Palaeoclimatol. Palaeoecol.* **286**, 202–217 (2010).
96. Irmis, R. B. & Whiteside, J. H. Delayed recovery of non-marine tetrapods after the end-Permian mass extinction tracks global carbon cycle. *Proc. R. Soc. Lond. B* **279**, 1310–1318 (2012).
97. Botha-Brink, J., Abdala, F. & Chinsamy-Turan, A. in *Forerunners of Mammals: Radiation, Histology, Biology* (ed Chinsamy-Turan, A.) 223–246 (Indiana Univ. Press, 2012).
98. Lloyd, G. T. & Slater, G. J. A total-group phylogenetic metatree for Cetacea and the importance of fossil data in diversification analyses. *Syst. Biol.* **70**, 922–939 (2021).
99. Lloyd, G. T. Estimating morphological diversity and tempo with discrete character–taxon matrices: implementation, challenges, progress, and future directions. *Biol. J. Linn. Soc.* **118**, 131–151 (2016).
100. R Core Team. *R: A Language and Environment for Statistical Computing* (R Foundation for Statistical Computing, 2021).
101. Goloboff, P. A., Farris, J. S. & Nixon, K. C. TNT, a free program for phylogenetic analysis. *Cladistics* **24**, 774–786 (2008).
102. Burgin, C. J., Colella, J. P., Kahn, P. L. & Upham, N. S. How many species of mammals are there? *J. Mammal.* **99**, 1–14 (2018).
103. Peters, S. E. & McClennen, M. The Paleobiology Database application programming interface. *Paleobiology* **42**, 1–7 (2016).
104. Kammerer, C. F., Angielczyk, K. D. & Frobisch, J. A comprehensive taxonomic revision of *Dicynodon* (Therapsida, Anomodontia) and its implications for dicynodont phylogeny, biogeography, and biostratigraphy. *J. Vertebr. Paleontol.* **11**, 1–158 (2011).
105. Bapst, D. W. paleotree: an R package for paleontological and phylogenetic analyses of evolution. *Methods Ecol. Evol.* **3**, 803–807 (2012).
106. Jones, K. E., Angielczyk, K. D. & Pierce, S. E. Stepwise shifts underlie evolutionary trends in morphological complexity of the mammalian vertebral column. *Nat. Commun.* **10**, 5071 (2019).
107. Pinheiro, J. et al. nlme: Linear and nonlinear mixed effects models, R package v.3.1–140 (2017); <https://CRAN.R-project.org/package=nlme>
108. Hörandl, E. Beyond cladistics: extending evolutionary classifications into deeper time levels. *Taxon* **59**, 345–350 (2010).
109. Lungmus, J. K. & Angielczyk, K. D. Phylogeny, function and ecology in the deep evolutionary history of the mammalian forelimb. *Proc. R. Soc. Lond. B* **288**, 20210494 (2021).
110. Brocklehurst, N. & Benson, R. B. J. Multiple paths to morphological diversification during the origin of amniotes. *Nat. Ecol. Evol.* **5**, 1243–1249 (2021).
111. Carroll, R. L. The earliest reptiles. *Zool. J. Linn. Soc.* **45**, 61–83 (1964).
112. Clavel, J., Escarguel, G. & Merceron, G. mvMORPH: an R package for fitting multivariate evolutionary models to morphometric data. *Methods Ecol. Evol.* **6**, 1311–1319 (2015).
113. Hansen, T. F. Stabilizing selection and the comparative analysis of adaptation. *Evolution* **51**, 1341–1351 (1997).
114. Burnham, K. P. & Anderson, D. R. *Model Selection and Multimodel Inference: A Practical Information-theoretic Approach* (Springer, 2002).
115. Paradis, E., Claude, J. & Strimmer, K. APE: analyses of phylogenetics and evolution in R language. *Bioinformatics* **20**, 289–290 (2004).

Acknowledgements

For discussions and feedback, we thank G. Slater, G. W. Mantilla, L. Weaver, S. Santana, K.-D. Benton, A. Bormet, C. Law and E. Panciroli. This work was funded by the National Science Foundation: DEB-1754502 (to K.D.A.) and DBI-1812126 (to D.M.G.).

Author contributions

S.M.H., D.M.G. and K.D.A. designed the study. S.M.H., G.T.L. and D.M.G. produced the metatree phylogeny. All authors (S.M.H., D.M.G., G.T.L., C.F.K. and K.D.A.) helped in collecting data and writing the paper. S.M.H. and D.M.G. performed analyses.

Competing interests

The authors declare no competing interests.

Additional information

Extended data is available for this paper at <https://doi.org/10.1038/s41559-023-02200-y>.

Supplementary information The online version contains supplementary material available at <https://doi.org/10.1038/s41559-023-02200-y>.

Correspondence and requests for materials should be addressed to Spencer M. Hellert.

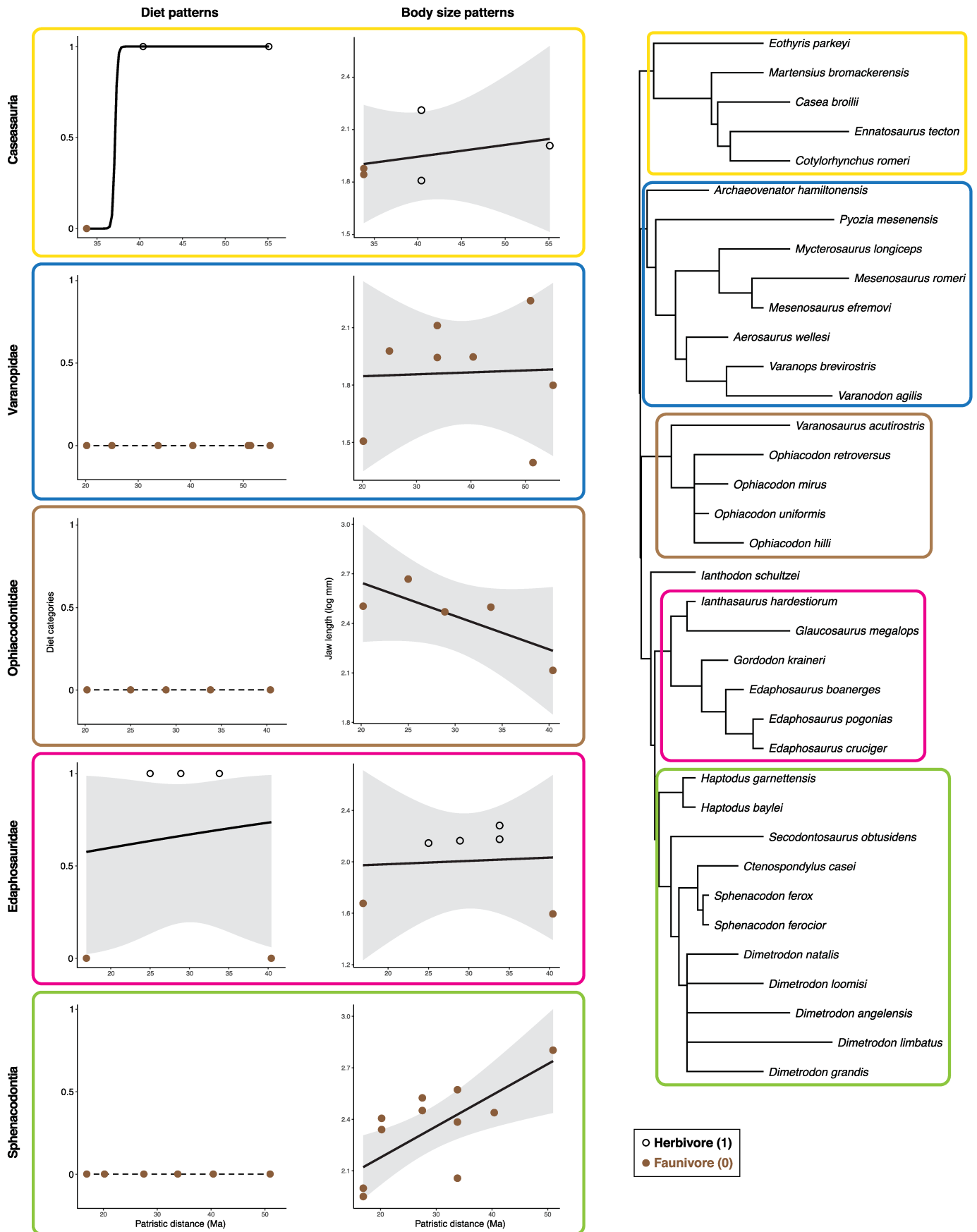
Peer review information *Nature Ecology & Evolution* thanks John Alroy and the other, anonymous, reviewer(s) for their contribution to the peer review of this work. Peer reviewer reports are available.

Reprints and permissions information is available at www.nature.com/reprints.

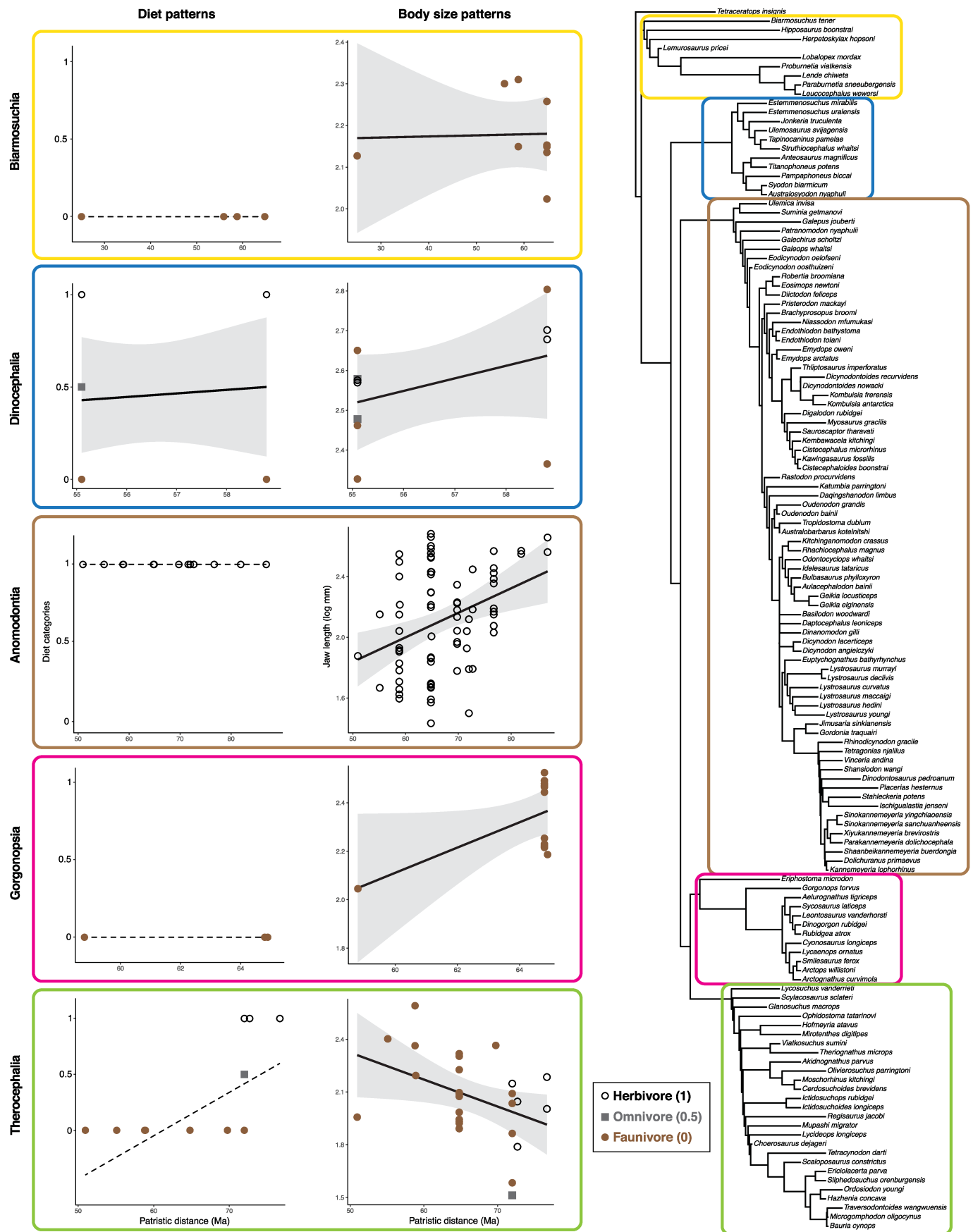
Publisher's note Springer Nature remains neutral with regard to jurisdictional claims in published maps and institutional affiliations.

Springer Nature or its licensor (e.g. a society or other partner) holds exclusive rights to this article under a publishing agreement with the author(s) or other rightsholder(s); author self-archiving of the accepted manuscript version of this article is solely governed by the terms of such publishing agreement and applicable law.

© The Author(s), under exclusive licence to Springer Nature Limited 2023



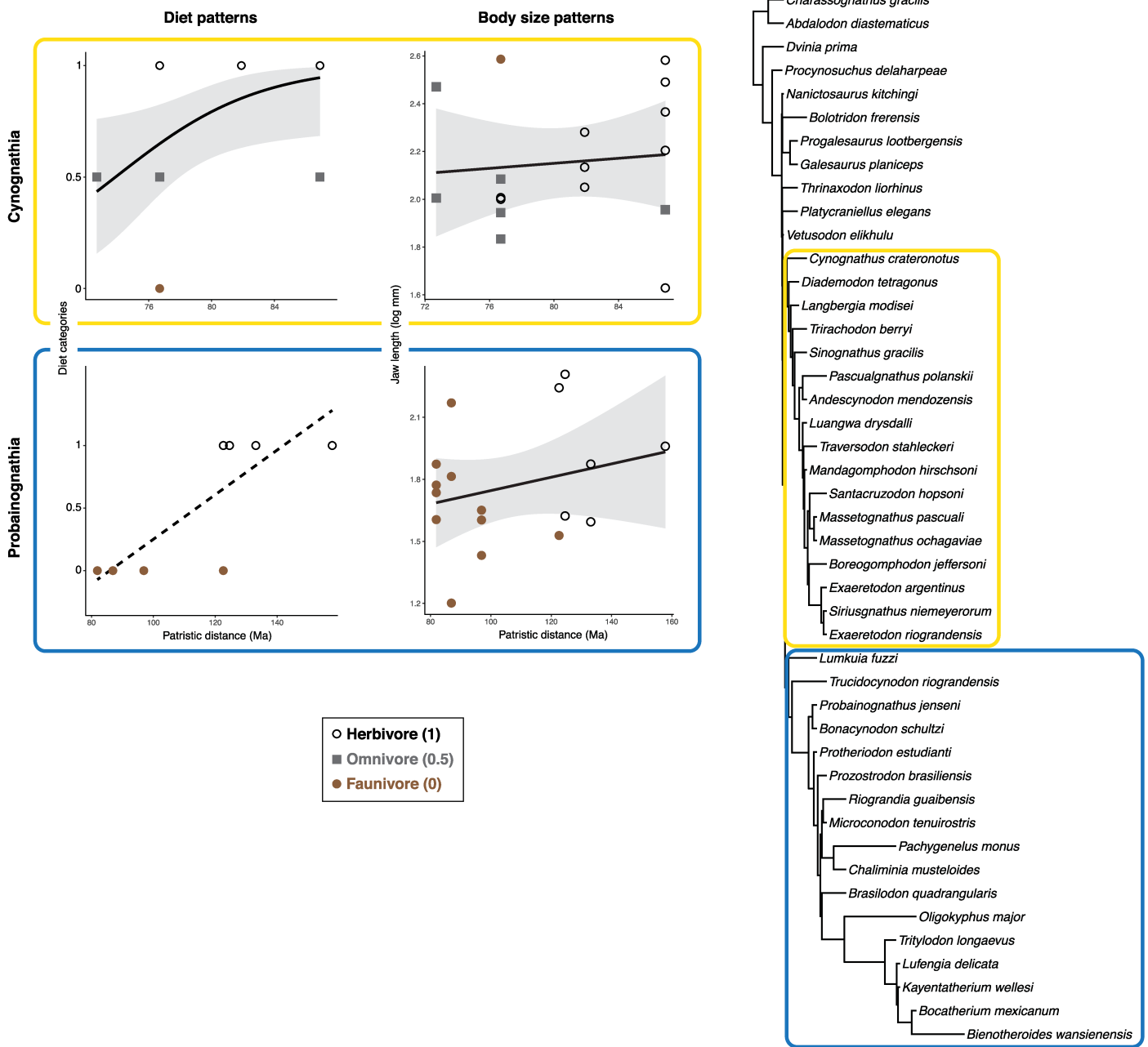
Extended Data Fig. 1 | Jaw length (\log_{10} mm) and diet regressed against patristic distance for pelycosaur subclades. The dashed lines are used for clades in which there is only a single diet. Grey bands are 95% confidence intervals.



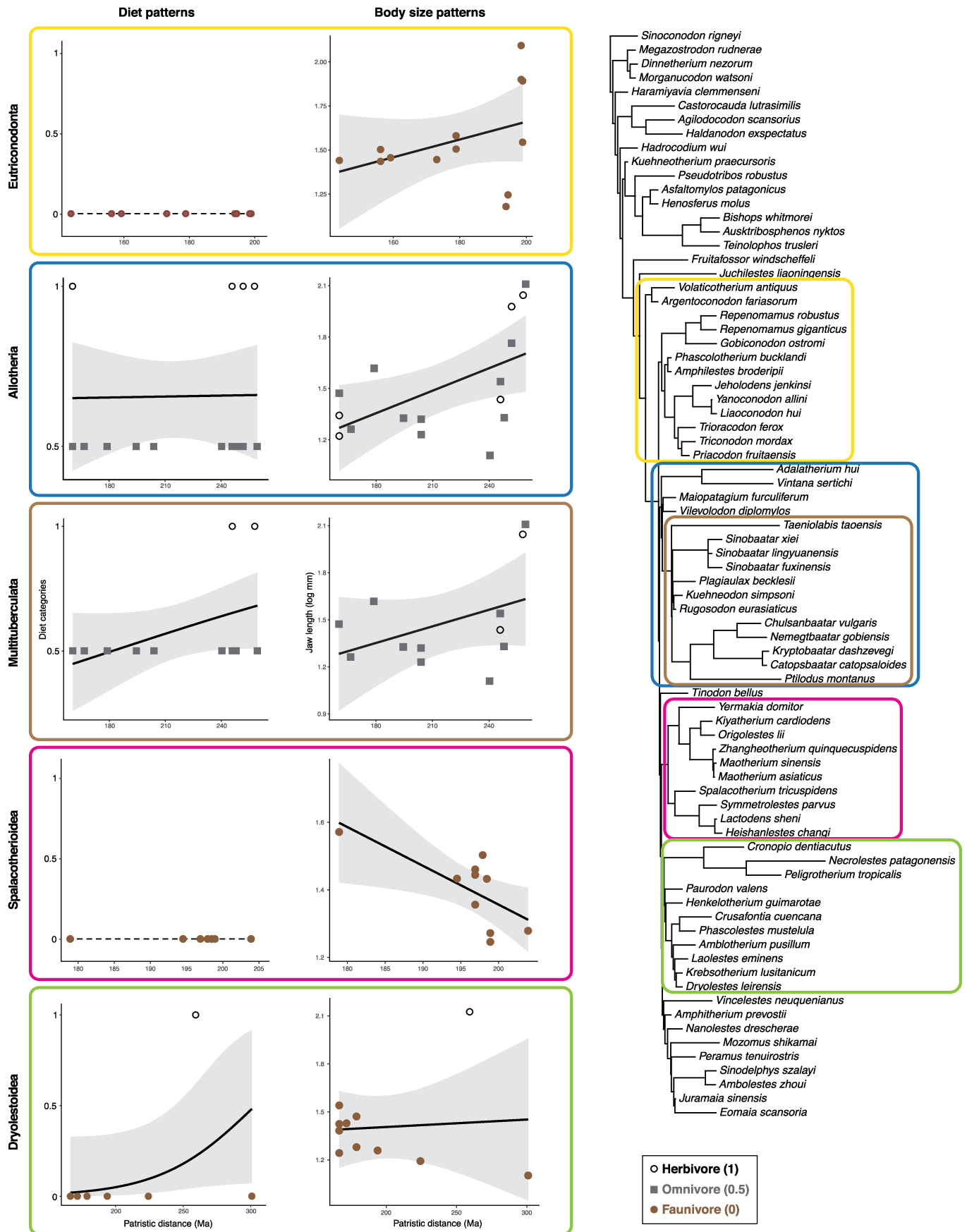
Extended Data Fig. 2 | See next page for caption.

Extended Data Fig. 2 | Jaw length (\log_{10} mm) and diet regressed against patristic distance for therapsid subclades. We do not include a quasibinomial model for Therocephalia because the model algorithm did not converge on a reasonable result; we instead present a linear model (dashed line). We did

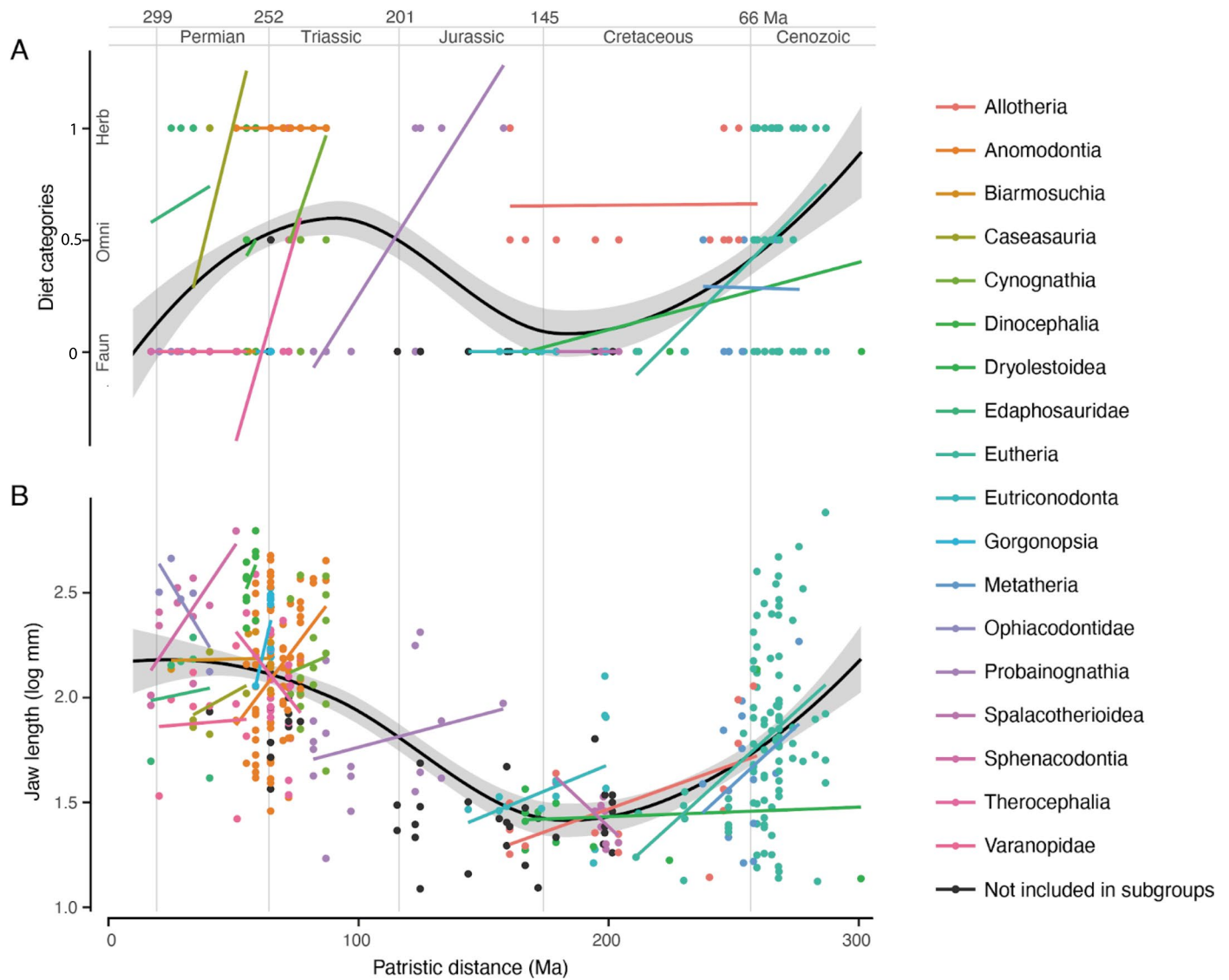
not fit regression models for diets of Biarmosuchia or Gorgonopsia because their members all have the same diets – the dashed lines are included to help emphasize the lack of diet change. Grey bands are 95% confidence intervals.



Extended Data Fig. 3 | Jaw length (log₁₀ mm) and diet regressed against patristic distance for cynodont subclades. We do not include a quasibinomial model for Probainognathia because the model algorithm did not converge on a reasonable result; we instead present a linear model (dashed line). Grey bands are 95% confidence intervals.

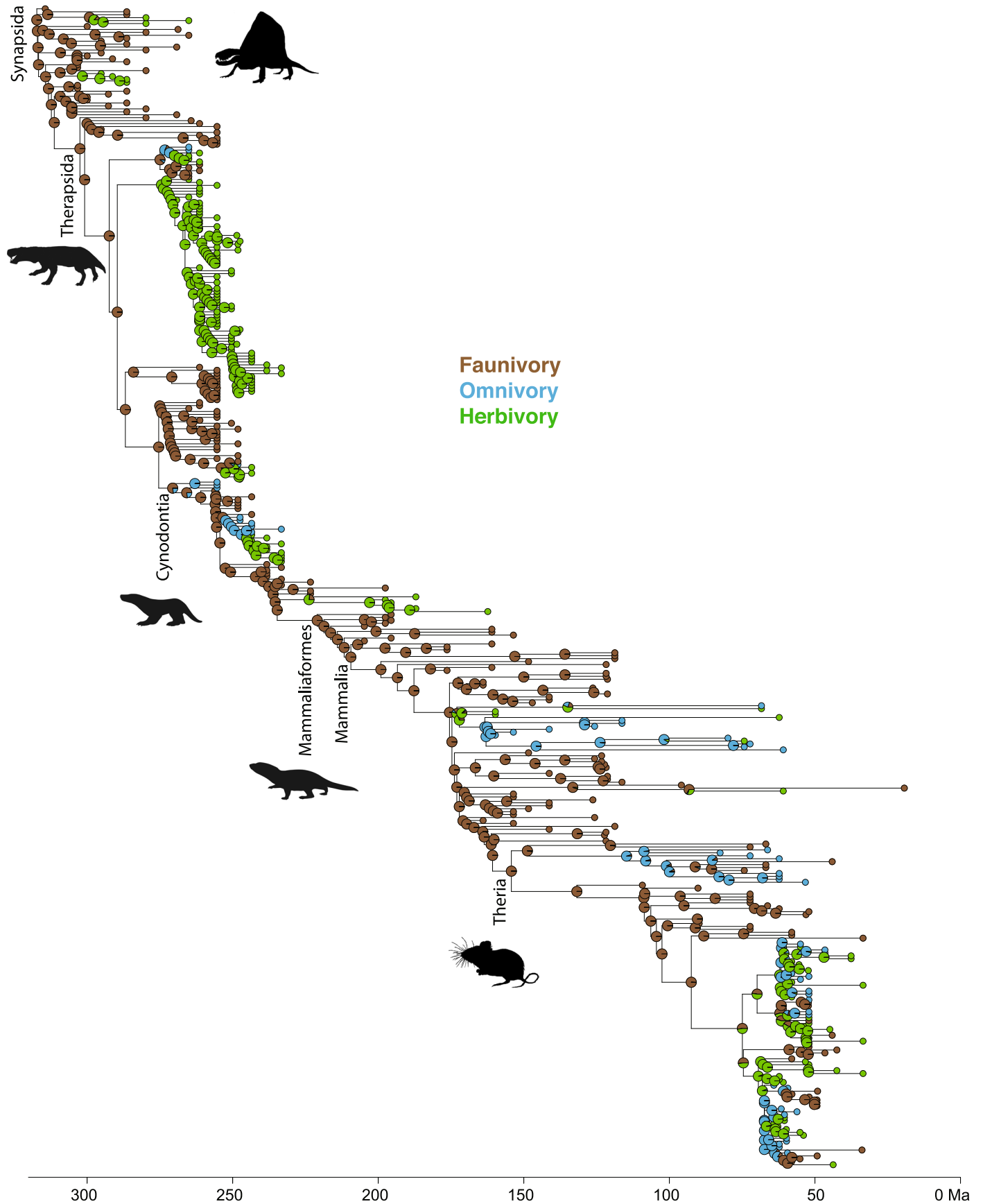


Extended Data Fig. 4 | Jaw length (\log_{10} mm) and diet regressed against patristic distance for mammaliaform subclades. The dashed lines are used for clades in which there is only a single diet. Grey bands are 95% confidence intervals.



Extended Data Fig. 6 | Diet (A) and jaw lengths (B) for all synsids in our sample are plotted against patristic distance. These are the similar plots to those in Figs. 1B and C, but the subclades (rather than five major radiations) are highlighted in this figure. The smaller, straight lines represent linear regressions for synsids subclades, and the grey curves are LOESS fitted regression curves (fitted to all data) and associated 95% confidence interval bands. For diet, we

plot linear models rather than quasibinomial models (such as in Fig. 2) because quasibinomial models could not be fit to many of the subclades (for example, see Extended Data Fig. 1–5). Multituberculates are not included in this plot as a separate group, but they are the major clade within Allotheria (Extended Data Fig. 4).



Extended Data Fig. 7 | Ancestral state reconstructions of discrete diets. The pie charts illustrate the scaled likelihood probabilities of the three diet categories. See Supplementary Fig. 1 for a phylogeny with tip labels, and see the Fig. 1 caption for silhouette sources.

Reporting Summary

Nature Portfolio wishes to improve the reproducibility of the work that we publish. This form provides structure for consistency and transparency in reporting. For further information on Nature Portfolio policies, see our [Editorial Policies](#) and the [Editorial Policy Checklist](#).

Statistics

For all statistical analyses, confirm that the following items are present in the figure legend, table legend, main text, or Methods section.

n/a Confirmed

- The exact sample size (n) for each experimental group/condition, given as a discrete number and unit of measurement
- A statement on whether measurements were taken from distinct samples or whether the same sample was measured repeatedly
- The statistical test(s) used AND whether they are one- or two-sided
Only common tests should be described solely by name; describe more complex techniques in the Methods section.
- A description of all covariates tested
- A description of any assumptions or corrections, such as tests of normality and adjustment for multiple comparisons
- A full description of the statistical parameters including central tendency (e.g. means) or other basic estimates (e.g. regression coefficient) AND variation (e.g. standard deviation) or associated estimates of uncertainty (e.g. confidence intervals)
- For null hypothesis testing, the test statistic (e.g. F , t , r) with confidence intervals, effect sizes, degrees of freedom and P value noted
Give P values as exact values whenever suitable.
- For Bayesian analysis, information on the choice of priors and Markov chain Monte Carlo settings
- For hierarchical and complex designs, identification of the appropriate level for tests and full reporting of outcomes
- Estimates of effect sizes (e.g. Cohen's d , Pearson's r), indicating how they were calculated

Our web collection on [statistics for biologists](#) contains articles on many of the points above.

Software and code

Policy information about [availability of computer code](#)

Data collection

Data analysis

For manuscripts utilizing custom algorithms or software that are central to the research but not yet described in published literature, software must be made available to editors and reviewers. We strongly encourage code deposition in a community repository (e.g. GitHub). See the Nature Portfolio [guidelines for submitting code & software](#) for further information.

Data

Policy information about [availability of data](#)

All manuscripts must include a [data availability statement](#). This statement should provide the following information, where applicable:

- Accession codes, unique identifiers, or web links for publicly available datasets
- A description of any restrictions on data availability
- For clinical datasets or third party data, please ensure that the statement adheres to our [policy](#)

Field-specific reporting

Please select the one below that is the best fit for your research. If you are not sure, read the appropriate sections before making your selection.

Life sciences Behavioural & social sciences Ecological, evolutionary & environmental sciences

For a reference copy of the document with all sections, see [nature.com/documents/nr-reporting-summary-flat.pdf](https://www.nature.com/documents/nr-reporting-summary-flat.pdf)

Ecological, evolutionary & environmental sciences study design

All studies must disclose on these points even when the disclosure is negative.

Study description	To examine macroevolutionary patterns in a phylogenetic context, we generated a time-calibrated meta-phylogeny ('metatree') comprising 2,128 synapsid species from the Carboniferous through the Eocene (305–34 Ma), based on 270 published character matrices. We used comparative methods to investigate body size and dietary evolution during successive synapsid radiations.
Research sample	<p>Metatree: For non-mammaliaform synapsids, we collected every morphological character matrix that has ever been published (to the best of our knowledge) as of July 2021 where non-mammaliaform synapsids composed the majority of the Operational Taxonomic Units (OTUs). We also collected the most comprehensive early mammaliaform matrices. We collected 269 matrices in total from 241 source studies (Supplementary Table 3). To time calibrate the majority rule topology, we began by querying the PBDB to obtain occurrence ages (Supplementary Table 4). We then vetted all PBDB age data, supplementing or updating them with biostratigraphic or radiometric age estimates from primary sources as much as possible.</p> <p>Body size proxies and dietary classifications: We collected jaw length measurements (as a proxy for body size) and dietary information for 404 synapsid species (37 pelycosaurs, 134 therapsids, 46 cynodonts, 80 mammaliaforms, and 110 therians). Jaws were measure from photographs taken by the authors and published figures in the literature (Supplementary Table 4). We used jaw length (log₁₀ mm) as a proxy for body size. Dietary information was taken from the PBDB and supplemented with information from the scientific literature whenever possible (Supplementary Table 3).</p>
Sampling strategy	Jaw length and dietary data were collected for as many taxa in our full metatree as possible. The availability of this information was based on the presence of appropriate photographs and dietary information in the literature.
Data collection	Jaw lengths were measured as the distance from the anterior tip of the dentary to the jaw joint/posterior condyle, parallel to the cheek tooth row (sensu Grossnickle 2020). We used jaw length (log ₁₀ mm) as a proxy for body size, in part because many different measurements have been used to approximate body size in different groups of synapsids (e.g. Wilson et al. 2012, Smits 2015, Sookias et al. 2012), making it challenging to produce consistent estimates across all synapsid groups. Jaw length measurements were collected by David Grossnickle and Christian Kammerer. Dietary information was taken from the PBDB and supplemented with information from the scientific literature whenever possible (Supplementary Table 3). This information was collected by David Grossnickle and Spencer Hellert.
Timing and spatial scale	The taxa in our dataset range from the Carboniferous through the Eocene (305–34 Ma). These dates were determined by the availability of jaw-length data, dietary data, and occurrence dates for the taxa with in our metatree.
Data exclusions	Jaw length data was excluded for juvenile individuals.
Reproducibility	The data we collected is available in the literature, but will also be available in a more concentrated format in the supplemental materials for the manuscript. This data can be easily reanalyzed using the openly available R packages we also used.
Randomization	We grouped taxa into one of three diet categories: 1) faunivores, 2) omnivores, or 3) herbivores. Insectivores, carnivores, and piscivores were included in the faunivore category.
Blinding	Blinding was not relevant this study.
Did the study involve field work?	<input type="checkbox"/> Yes <input checked="" type="checkbox"/> No

Reporting for specific materials, systems and methods

We require information from authors about some types of materials, experimental systems and methods used in many studies. Here, indicate whether each material, system or method listed is relevant to your study. If you are not sure if a list item applies to your research, read the appropriate section before selecting a response.

Materials & experimental systems

n/a	Involvement in the study
<input checked="" type="checkbox"/>	<input type="checkbox"/> Antibodies
<input checked="" type="checkbox"/>	<input type="checkbox"/> Eukaryotic cell lines
<input type="checkbox"/>	<input checked="" type="checkbox"/> Palaeontology and archaeology
<input checked="" type="checkbox"/>	<input type="checkbox"/> Animals and other organisms
<input checked="" type="checkbox"/>	<input type="checkbox"/> Human research participants
<input checked="" type="checkbox"/>	<input type="checkbox"/> Clinical data
<input checked="" type="checkbox"/>	<input type="checkbox"/> Dual use research of concern

Methods

n/a	Involvement in the study
<input checked="" type="checkbox"/>	<input type="checkbox"/> ChIP-seq
<input checked="" type="checkbox"/>	<input type="checkbox"/> Flow cytometry
<input checked="" type="checkbox"/>	<input type="checkbox"/> MRI-based neuroimaging

Palaeontology and Archaeology

Specimen provenance	No specimens were collected for this study. All data came from published studies.
Specimen deposition	No specimens were collected for this study. All data came from published studies.
Dating methods	All data came from published studies.
<input checked="" type="checkbox"/> Tick this box to confirm that the raw and calibrated dates are available in the paper or in Supplementary Information.	
Ethics oversight	No ethical approval or guidance was necessary. This is because no specimens were collected for this study. All data came from published studies.

Note that full information on the approval of the study protocol must also be provided in the manuscript.